Monitoring of Actin Unfolding by Room Temperature Tryptophan Phosphorescence†

Vladimir M. Mazhul',‡ Ekaterina M. Zaitseva,‡ Mikhail M. Shavlovsky,§ Olesia V. Stepanenko,# Irina M. Kuznetsova,# and Konstantin K. Turoverov*,#

Institute of Photobiology, National Academy of Sciences of Belarus, Minsk 220072, Belarus, Institute for Experimental Medicine, Russian Academy of Medical Sciences, St. Petersburg 197376, Russia, and Institute of Cytology, Russian Academy of Sciences, St. Petersburg 194064, Russia

Received June 16, 2003; Revised Manuscript Received September 22, 2003

ABSTRACT: Slow intramolecular mobility of native and inactivated actin from rabbit skeletal muscle during the process of protein unfolding induced by GdnHCl was studied using tryptophan room temperature phosphorescence (RTP). By this method, the conclusion was confirmed that an essentially unfolded intermediate preceded the formation of inactivated actin [Turoverov et al. *Biochemistry* (2002) *41*, 1014−1019]. It was found that the kinetic intermediate generated at the early stage of protein denaturation has no tryptophan RTP, suggesting the high lability of its structure. Symbate changes of integral intensity and the mean lifetime of RTP during the U* → I transition suggests a gradual increase of the number of monomers incorporated in the associate ($U^* \rightarrow I_1 \cdots \rightarrow I_n \cdots \rightarrow I_{15}$), which is accompanied by an increase of structural rigidity. The rate of inactivated actin formation ($I \equiv I_{15}$) is shown to increase with the increase of protein concentration. It is shown that, no matter what the means of inactivation, actin transition to the inactivated state is accompanied by a significant increase of both integral intensity and the mean lifetime of RTP, suggesting that inactivated actin has a rigid structure.

The problem of protein folding to a compact, highly ordered, functionally active state is one of the central problems of modern structural and cell biology. Characterization of the unfolding−refolding process as well as intermediate and misfolded states appearing on these pathways is considered an important strategy in studying this problem. Such studies are not only of fundamental importance for solving the problem of the protein folding, but also have a practical significance for medicine (in connection with the existence of the so-called conformational diseases caused by amyloid fibril formation that results from protein folding abnormalities; *1*−*8*) and biotechnology (in connection with the appearance of misfolded protein aggregates and their accumulation in inclusion bodies; *8*−*13*). Equilibrium intramolecular mobility which is realized in a wide time range from 10^{-14} to 10 s plays an important role in protein functioning and folding (*14*−*20*).

Strong dependence of tryptophan residues phosphorescence lifetimes and quantum yields on the mobility of their microenvironments, as well as a long lifetime of room temperature phosphorescence (RTP)[1] of tryptophan residues permits the monitoring of intramolecular mobility of proteins in the wide time scale range, with relaxation times up to milliseconds (*19*−*28*).

The goal of this work was to study slow intramolecular mobility of actin in different structural states and its changes during GdnHCl-induced formation of inactivated actin. The globule of monomer actin (G-actin) is formed by a single polypeptide chain containing 375 amino acids (molecular mass is 42 kDa). Actin monomer consists of two domains, each comprising two subdomains (*29*). All four tryptophan residues are located in subdomain I. Actin monomer contains one rigidly tied calcium cation and one ATP molecule. As a result of polymerization, G-actin is transformed into a fibrous form called F-actin. In 1972, Lehrer and Kerwar (*30*) showed that the removal of calcium cation leads to irreversible transformation of G-actin into a denaturated state, in which the protein is unable to polymerize. The protein in this state was called inactivated actin. Later, it was demonstrated that inactivated actin could be obtained not only as a result of Ca^{2+} removal, but also by a heat treatment (60−70 °C), by incubation with a moderate concentration of urea (3−4 M) or GdnHCl (0.8−1.8 M), by dialysis from 8 M urea or 6 M GdnHCl, and even spontaneously during a prolonged storage (*30*−*39*). Inactivated actin is a thermodynamically stable monodispersed associate composed of 15 monomer units (*40*). Properties of inactivated actin do not depend on the method of denaturation (*31*, *41*). A peculiar feature of inactivated actin is restriction of intramolecular

† This work was supported in part by Grants B02P-077 from the Belorussian Foundation of Basic Research, and 02−04−81013 from the Russian Foundation of Basic Research, a grant from Presidium of Russian Academy of Science on the Program "Physicochemical Biology", and Grant INTAS-2001-2347.

* To whom correspondence should be addressed: Institute of Cytology RAS, Tikhoretsky Ave., 4, 194064 St. Petersburg, Russia. Fax: 7(812)247−0341. E-mail: kkt@mail.cytspb.rssi.ru.

‡ National Academy of Sciences of Belarus.

§ Russian Academy of Medical Science.

Russian Academy of Science.

[1] Abbreviations: RTP, room temperature phosphorescence; GdnHCl, guanidine hydrochloride; CD, circular dichroism; UV, ultraviolet; EDTA, ethylenediaminetetraacetic acid; ATF, adenosine 5′-triphosphate.

10.1021/bi0350295 CCC: $25.00
Published on Web 10/29/2003

mobility of tryptophan residues (results of anisotropy of tryptophan fluorescence) and their microenvironments (results of CD in near UV-spectra) in comparison with that in G-actin (*31*, *41*). Recently, it has been established that inactivated actin is not intermediate between the native and completely unfolded state (*42*). Tryptophan fluorescence and CD kinetic studies of GdnHCl-induced actin unfolding have demonstrated that native actin N is transformed into the inactivated state I not directly, but via an intermediate stage characterized by formation of the essentially unfolded kinetic intermediate U* (*43*). In contrast to the completely unfolded state, actin in the essentially unfolded state U* preserves its secondary structure to a great extent. This structural state of the protein was defined as the "premolten globule". The essentially unfolded state U* can appear not only as a result of the native protein denaturation, but also upon refolding from the completely unfolded state U (*43*).

Spectral and kinetic characteristics of tryptophan phosphorescence of actin at low and room temperatures has been studied (*44*, *45*), yet RTP has not been used for monitoring the change of slow intramolecular mobility at different stages of actin denaturation. The use of tryptophan RTP in studies of actin unfolding kinetics allow further specification of the actin folding−unfolding model that was proposed earlier and characterization of the slow intramolecular mobility in different structural states.

MATERIALS AND METHODS

Preparations. Rabbit skeletal muscle actin was purified by the standard procedure (*46*). G-actin in buffer G (0.2 mM ATP, 0.1 mM $CaCl_2$, 0.4 mM β-mercaptoethanol, 5 mM Tris-HCl, pH 8.2, and 1 mM NaN_3) was stored on ice and used within 1 week. Actin was purified by one or two cycles of polymerization−depolymerization, using 30 mM KCl for polymerization. The nativity of samples was characterized by the parameter $A = (I_{320}/I_{365})_{297}$, where I_{320} and I_{365} are fluorescence intensities at $\lambda_{em} = 320$ and 365 nm, respectively, and $\lambda_{ex} = 297$ nm (*47*). Samples with the *A* parameter not lower than 2.56, which corresponds to the content of inactivated actin not higher than 2% (*47*), were used. Actin concentration was determined with a Hitachi spectrophotometer (Japan). The molar extinction constant for actin was taken as $E_{280} = 1.09$ mg^{-1} mL cm^{-1} (*48*). The concentration of GdnHCl was determined by measuring the refractive index of its solution with an Abbe refractometer (LOMO, Russia).

Inactivated actin was obtained from G-actin by the Ca^{2+} cation removal by dialysis of the protein solution for 20 h against the buffer containing 5 mM EDTA, incubation at 70 °C for 30 min, incubation with 3−4 M urea or with 1−2 M GdnHCl, and dialysis from 6 M GdnHCl solution for 20 h. The final actin concentration varied from 0.8 to 2.5 mg/mL. Deoxygenation of the samples was performed by addition of sodium sulfide to a final concentration of 50 mM (*26*, *27*). The use of sodium sulfide for deoxygenation for RTP investigations is also described in refs *49* and *50*. Residual oxygen concentration did not exceed 1 nM. Complete deoxygenation took 7 min.

All chemicals were of reagent grade or better. GdnHCl (Nacalai Tesque, Japan) was used without additional purification.

Phosphorescence Measurements. Phosphorescence measurements of deoxygenated protein samples were carried out at 20 °C, using a highly sensitive homemade device with monochrome excitation and registration of emission, as described elsewhere (*51*, *52*). The phosphoroscope dead time was 1 ms. Tryptophan phosphorescence was excited at 297 nm. RTP decays were recorded at 445 nm. Phosphorescence spectra were corrected for instrumental response.

Data analysis. Phosphorescence decays were analyzed in terms of a sum of discrete exponential components by a nonlinear least-squares fitting algorithm implemented by the program Fotobio (Department of System Analysis, Belorussian State University). In all cases, two decay times (eq 1) gave the best fit.

$$I(t)/I_0 = \alpha_1 \exp(-t/\tau_1) + \alpha_2 \exp(-t/\tau_2) \qquad (1)$$

where $I(t)$ is the phosphorescence intensity, I_0 is the initial phosphorescence intensity ($t = 0$), τ_1 is the lifetime of the fast component, τ_2 is the lifetime of the slow component, α_1 and α_2 are amplitudes of the fast and slow components, respectively ($\alpha_1 + \alpha_2 = 1$).

The analysis was determined to be adequate if the reduced chi-squared, χ^2, was close to unity and the visual inspection of weighted residuals and autocorrelation plots showed a random dispersion centered around zero.

The integral phosphorescence intensity was calculated from the areas under the RTP decay curve according to

$$I_{int} = I_0(\alpha_1 \int_0^\infty \exp(-t/\tau_1)dt + \alpha_2 \int_0^\infty \exp(-t/\tau_2)dt) = I_0(\alpha_1\tau_1 + \alpha_2\tau_2) = I_0\bar{\tau} \qquad (2)$$

here $\bar{\tau}$ is the simple mean of the RTP lifetime. The contribution of the fast component to the total emission S_1 was calculated as follows:

$$S_1 = \frac{\alpha_1 \int_0^\infty \exp(-t/\tau_1)dt}{\alpha_1 \int_0^\infty \exp(-t/\tau_1)dt + \alpha_2 \int_0^\infty \exp(-t/\tau_2)dt} = \frac{\alpha_1\tau_1}{\alpha_1\tau_1 + \alpha_2\tau_2} \qquad (3)$$

The mean weighted RTP lifetime $<\tau>$ was calculated as follows:

$$\langle\tau\rangle = \frac{\alpha_1{\tau_1}^2 + \alpha_2{\tau_2}^2}{\alpha_1\tau_1 + \alpha_2\tau_2} \qquad (4)$$

All results reported are the means of three or more independent measurements.

RESULTS

RTP emission spectra of G-actin, F-actin, and inactivated actin have maxima at 417, 445, and 470 nm, and are practically identical in shape (Figure 1). The RTP decay kinetics of G-actin, F-actin, and inactivated actin are well approximated by the sum of two exponentials. Figure 2 shows the RTP decay kinetics of G-actin and inactivated actin. The characteristics of RTP (τ_1, τ_2, $<\tau>$, α_1, S_1) for G-, F-, and inactivated actin are summarized in Table 1. The obtained values of the RTP lifetimes and amplitude of G- and F-actin agree well with the data reported by Strambini and Lehrer (*45*). Actin polymerization leads to an increase

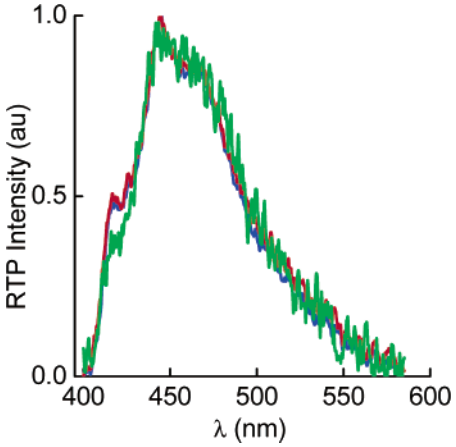

FIGURE 1: Phosphorescence spectra of actin. Spectra of G-, F-actin, and inactivated actin are designated in red, blue, and green, respectively. Inactivated actin was obtained as a result of incubation of G-actin with 1.8 M GdnHCl for 24 h. All spectra were normalized to the intensity at maximum 445 nm and corrected for instrumental response. Protein concentration was 1.5 mg/mL. λ_{ex} = 297 nm.

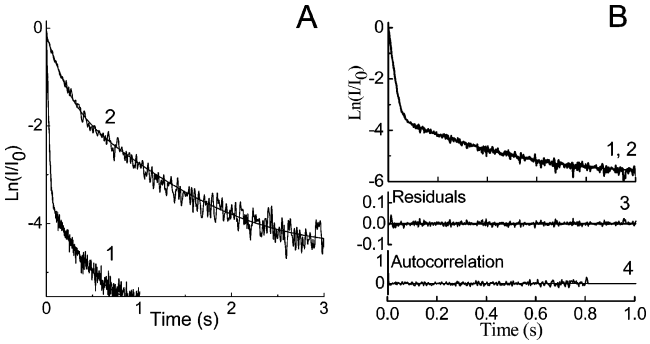

FIGURE 2: Phosphorescence decay curves of actin. (A) Phosphorescence decay curve of native (1) and inactivated in 1.5 M GdnHCl (2) actin. (B) Phosphorescence decay curve of G-actin alongside with a fitted curve and residuals functions. Experimental data (curve 1), a fitting to a biexponential law (curve 2), weighted residuals (curve 3), and an autocorrelation function of the weighted residuals (curve 4). Protein concentration was 1.5 mg/mL, λ_{ex} = 297 nm, λ_{em} = 445 nm.

of the slow component and its contribution to the bulk phosphorescence, while the fast component remains virtually unchanged (Table 1). It was found that the lifetime of RTP of inactivated actin was much longer than that of its native form, regardless of the method used for actin denaturation. Moreover, both τ_1 and τ_2 increased, and their contribution to the bulk phosphorescence changed. Unlike G- and F-actin, the major contribution to phosphorescence of inactivated actin is provided by the slower component.

Figure 3 (panels A and B) shows kinetic dependencies of mean lifetimes and integral intensity of RTP of actin at different concentrations, when actin unfolding was induced by 1.8 M GdnHCl. The beginning of RTP measurements was limited by the dead time required for solution deoxygenation, which amounted to about 7 min. It was found that for a protein concentration of 0.8 mg/mL for the first minutes of the phosphorescence measurement, RTP of actin was below the detection limits; the low-intensity actin RTP appeared thereafter. At subsequent incubation in the GdnHCl solution the values of RTP $<\tau>$ and I_{int} increased and reached their maxima in approximately 70 min (Figure 3). At higher protein concentrations (1.0−2.5 mg/mL), the actin

Table 1: Room Temperature Phosphorescence of G-actin, F-actin, and Inactivated Actin[a]

actin state structure, experimental conditions	τ_1, ms	τ_2, ms	$<\tau>$, ms	α_1	S_1
G-actin	12	251	122	0.96	0.53
F-actin	13	260	129	0.96	0.54
inactivated actin, Ca^{2+} removal	71	403	303	0.71	0.30
inactivated actin, 70 °C, incubation for 30 min	71	428	321	0.72	0.30
inactivated actin, 1.5 M GdnHCl, incubation for 24 h	73	410	319	0.67	0.26
inactivated actin, dialysis for 20 h from 6 M GdnHCl	72	420	331	0.67	0.26
inactivated actin, 4 M urea, incubation for 24 h	65	390	311	0.66	0.25

[a] Lifetime (τ_1,τ_2) and preexponential amplitude (α_1) of the short-lived decay component were obtained from a biexponential fitting of phosphorescence decay of the actin solutions. The contribution of the short-lived decay component to the total emission (S_1) and average phosphorescence lifetime ($<\tau>$) were calculated from eqs 3 and 4, accordingly. The data are averages of five independent experiments. Reproducibility is typically better than 7%.

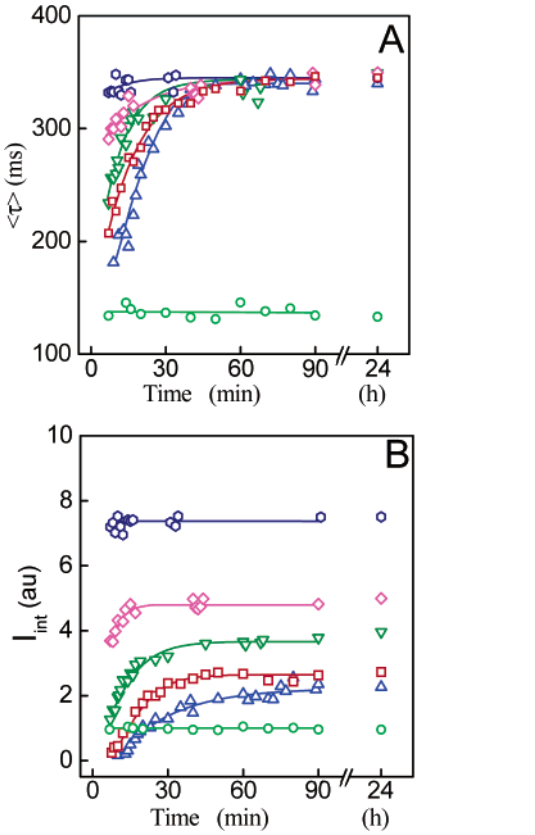

FIGURE 3: Kinetics of actin denaturation induced by 1.8 M GdnHCl. (A) Kinetics of the change of the mean RTP lifetime. (B) Kinetics of the change of RTP integral intensity. Concentrations of actin are (mg/mL): blue up triangles − 0.8; red squares − 1.0; green down triangles − 1.5; magenta diamonds − 2.0; blue hexagons − 2.5; RTP parameters of native actin (1 mg/mL) designated as green circles. λ_{ex} = 297 nm, λ_{em} = 445 nm.

RTP was reliably detected immediately after the deoxygenation procedure, i.e., after 7 min of the protein incubation in 1.8 M GdnHCl. The maximal values of $<\tau>$ and I_{int} were reached much faster. After reaching their maxima, the values of $<\tau>$ and I_{int} remained constant at further incubation. It was discovered that the maximum value of $<\tau>$ of RTP of actin in 1.8 M GdnHCl did not depend on protein concentration, whereas I_{int} did.

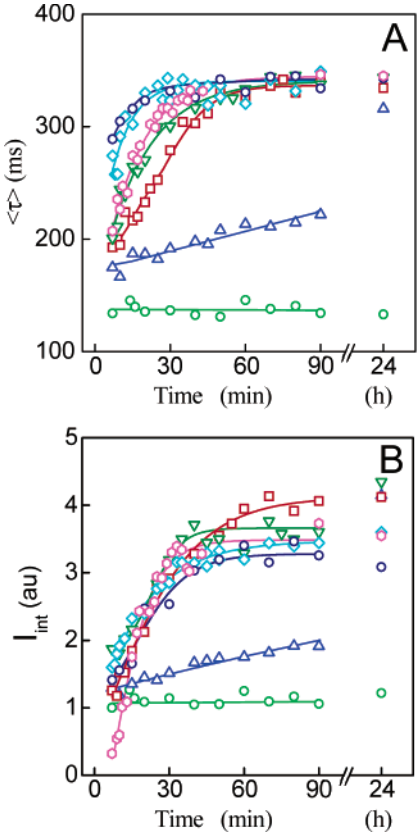

FIGURE 4: Kinetics of actin denaturation induced by different concentration of GdnHCl. (A) Kinetics of the change of the mean RTP lifetime. (B) Kinetics of the change of RTP integral intensity. Final concentrations of GdnHCl (M) are green circles − 0; blue up triangles − 0.5; red squares − 0.7; green down triangles − 1.0; magenta hexagons − 1.2; cyan diamonds − 1.5; blue circles − 1.8. Protein concentration was 1.0 mg/mL, λ_{ex} = 297 nm, λ_{em} = 445 nm.

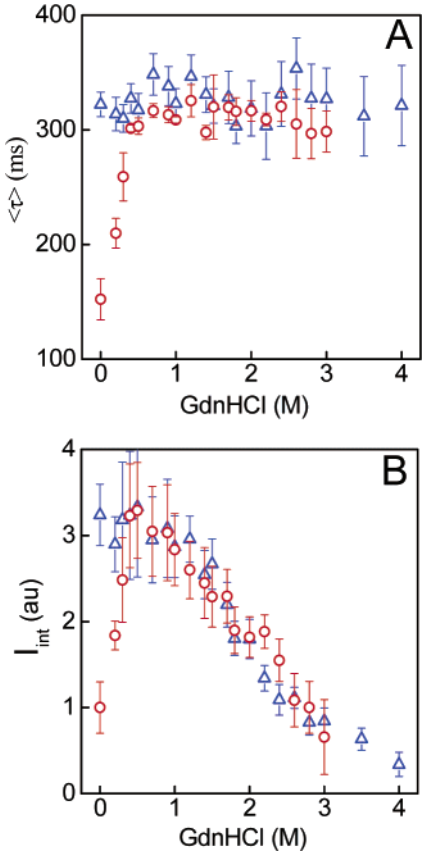

FIGURE 5: Dependencies of tryptophan RTP of native (red circles) and previously inactivated (blue triangles) actin on GdnHCl concentration. (A) The mean RTP lifetime. (B) Integral RTP intensity. Protein concentration was 1.5 mg/mL, λ_{ex} = 297 nm, λ_{em} = 445 nm.

Figure 4 shows kinetic curves of the mean lifetimes and integral intensities of RTP of actin at the same concentration (1 mg/mL), when the actin unfolding was induced by GdnHCl solutions at different concentrations. It is evident that the rate of reaching the maximal values of $<\tau>$ and I_{int} depends on GdnHCl concentration. At low concentration of GdnHCl, the maximal value of $<\tau>$ was not reached even after an overnight incubation.

Figure 5 shows stationary dependencies of RTP characteristics of actin on GdnHCl concentration in the solution obtained for the initially native (red circles) and initially inactivated (blue circles) actin. It was established that in the range of GdnHCl concentrations from 0.8 to 4.0 M the values of τ_1, τ_2, and α_1 (data are not shown) and $<\tau>$, and I_{int} of RTP practically coincided for the initially native and initially inactivated actin solutions. In the range of GdnHCl concentrations from 0 to 0.8 M, all characteristics of RTP for the initially native and initially inactivated actin solutions differ statistically significantly. In this range, the dependence for initially native actin is quasi-stationary, as at low concentrations of GdnHCl the RTP values did not reach their maxima even after an overnight incubation. At GdnHCl concentrations exceeding 3 M RTP the intensity became so low that any further measurement was not possible. Meanwhile, for initially inactivated actin, RPT can be reliably recorded up to 4 M GdnHCl concentration.

DISCUSSION

In the absence of molecular oxygen, most proteins have been found to phosphoresce in aqueous solution at room temperature (*22*−*24*). Quantum yield (q_p) and consequently integral intensity of phosphorescence depends in a complicated way on certain photophysical processes that occur both in triplet and in singlet states, whereas the lifetime of phosphorescence is determined by rate constants of radiative and nonradiative processes of the triplet state (*22*, *53*).

The dominating quenching mechanism of tryptophan phosphorescence in the oxygen-free medium is deactivation of triplet-exited states due to collisions of the indole ring of a tryptophan residue with the surrounding structural elements of macromolecules. The frequency and energy of these collisions resulting in out-of-plane vibrations of the indole ring and relaxation of triplet states define the efficiency of dynamic quenching of the tryptophan phosphorescence. If tryptophan residues are located within rigid parts of the protein globule with a high microenvironment packing density, the typical RTP lifetime is in the range from 1 to 2 s to hundreds of milliseconds. It is in such an environment, whose rigidity is similar to that of a crystal, that the tryptophan residue Trp 109 of *Escherichia coli* alkaline phosphatase is located ($\tau \approx 2$ s). The RTP lifetime of residues located in more mobile environments is reduced down to values from several tens of milliseconds to 1−0.5 ms. The triplet-excited states of tryptophan residues located at the periphery of the globule in the highly mobile environment

are deactivated mainly via a nonradiative mechanism resulting in the effective dynamic quenching of RTP, which considerably decreases the decay times (*19*−*28*).

Along with the dynamic quenching of the tryptophan phosphorescence, static quenching may be present, which takes place when the indole ring of a tryptophan residue is in close contact with side chains of some phosphorescence-quenching amino acids. By their ability to quench tryptophan phosphorescence, the side chains of amino acids can be divided into three classes: (i) strongly quenching ($k_q \approx 5 \times 10^8$ M^{-1} s^{-1}), such as cysteine; (ii) intermediately quenching ($k_q = 5 \times 10^5 - 2 \times 10^7$ M^{-1} s^{-1}), such as tyrosine, histidine, and tryptophan; (iii) weakly quenching or nonquenching ($k_q \leq 10^5$ $M^{-1}s^{-1}$), all other amino acid residues (*23*). Static quenching of RTP by side chains of cysteine, tyrosine, and tryptophan is possible only if the distance between the indole ring and the quenching group is comparable to the van der Waals radius (i.e., does not exceed several angstroms).

A special role in the intramolecular quenching is played by disulfide groups. Their pronounced ability to quench RTP is due to their capability to accept electron from tryptophan in the triplet-exited state (*24*, *54*, *55*). Intramolecular quenching may occur not only if the indole ring is in permanent contact with the quenching amino acid residue (static quenching), but also if it is transiently brought into contact with the quencher by protein structural fluctuations (*23*). Consequently, efficiency of the quenching action of groups that are potential quenchers of phosphorescence, located in the vicinity of the indole ring, is also determined to a great extent by intramolecular mobility of the chromophore microenvironment. The quenching efficiency depends not only on the distance between the tryptophan residue and the quenching group, but also on its orientation relative to the tryptophan residue indole ring. Therefore, the presence of the potential RTP quenching residues in the tryptophan residue microenvironment does not necessarily result in phosphorescence quenching. Because of the difficulty of taking into account all factors causing the triplet-exited state deactivation, it is not always possible to precisely define parameters of phosphorescence of individual tryptophan residues in multitryptophan proteins.

Room Temperature Tryptophan Phosphorescence of Inactivated Actin. As mentioned above, actin inactivation leads to a considerable increase in RTP lifetime. A several fold increase of τ_1, τ_2, and $<\tau>$ values of the actin RTP after the 24-h protein incubation with 1.8 M GdnHCl indicates a reduction of the protein internal mobility at locations of RTP-capable tryptophan residues. The most probable reason for this increase of the tryptophan residue microenvironment is stabilization of the inactivated actin structure due to association of partially folded macromolecules. It was shown earlier that inactivated actin is a thermodynamically stable monodisperse associate with the sedimentation constant 20 S, consisting of 15 monomeric units (*31*, *40*). An increase of τ of RTP after the protein associate formation was reported earlier in studies of muscle glycogen phosphorylase *b* (*26*). It is important that according to the RTP parameters obtained, values of intramolecular mobility of inactivated actin obtained with different methods are rather similar. The existence of RTP is in line with the pronounced signal in the near UV CD spectrum. Both suggest the low mobility of the tryptophan residue microenvironment in inactivated actin (*31*, *41*).

The dependencies of τ_1, τ_2, α_1 (not shown), $<\tau>$, and I_{int} (Figure 5A) on GdnHCl concentration for the initially native and initially inactivated actin in the range of GdnHCl concentrations from 0.8 to 1.8 M almost coincide. At a concentration of GdnHCl lower than 0.8 M the values of τ_1, τ_2, $<\tau>$, and I_{int} are lower, while that of α_1 are higher for the initially native than for the initially inactivated actin. This is because in this range of GdnHCl concentrations the values of these RTP characteristics of the initially native actin are quasi-stationary and do not reach their equilibrium values, which are characteristic of inactivated actin, even after incubation at these GdnHCl concentrations overnight and longer. The values of τ_1 and τ_2 of the initially inactivated actin decrease slightly with increase of GdnHCl concentration in the range from 0 to 1.8 M (data are not shown). Due to the redistribution of the contribution of the fast and slow components, the mean values of the phosphorescence decay time remain constant in this range of GdnHCl concentrations. The fluorescence intensity and the value of parameter *A* characterizing the spectrum position decrease slightly with the increase of the GdnHCl concentration from 0 to 1.8 M (*41*, *42*). At the same time, the integral phosphorescence intensity significantly decreases with the increase of the GdnHCl concentration from 0.8 to 1.8 M (Figure 5B). This decrease is so pronounced that on its background the change of integral intensity of the phosphorescence caused by the inactivated actin unfolding at GdnHCl concentrations in the range from 1.8 to 3.5 M cannot be observed clearly. At present, it is hard to explain unambiguously the significant decrease of I_{int} with the increase of the GdnHCl concentration, while phosphorescence decay time changes only slightly under the same conditions. On the other hand, this is not entirely surprising, as the phosphorescence decay time is determined only by the processes of the triplet state, whereas the integral RTP intensity is determined by the processes of both the triplet and singlet state.

The significant change of the integral intensity of RTP from the concentration of GdnHCl in the range of concentration from 0.8 to 1.8 M cannot be explained by the change of protein structure. It is shown by intrinsic fluorescence and CD (*41*). This phenomenon cannot be explained by dynamic quenching of RTP due to the increase of structural mobility because RTP lifetime remains constant in this range of GdnHCl concentration. It also cannot be explained by the process in singlet state because fluorescence intensity (*31*) and fluorescence lifetime (unpublished data) change *insignificantly* in this range of GdnHCl concentration. The possible explanation of this phenomenon is the existence, together with inter system crossing, of the alternative way of triplet level populating which arises from geminate recombination of the indole radical cation and solvated electron (*53*). One can assume that the change of GdnHCl concentration significantly affects the structure of the solvent and thus causes changes in the probability of the appearance and recombination of the indole radical cation and solvated electron. Another possible explanation could be provided by the changes of inactivated actin structure (disintegration of aggregate) with the increase of GdnHCl concentration. The examination of this assumption is in progress.

Integral intensity of the completely unfolded RTP of actin is equal to zero. Therefore, the integral intensity is reduced, while the RTP decay time remains constant, equal to that of inactivated actin, with decrease of the inactivated actin portion in the range of the inactivated actin unfolding (1.8−3.5 M GdnHCl). It was shown earlier that the process of the initially inactivated actin unfolding is very slow when it is transferred to 4 M GdnHCl (*43*) and even after 24 h of incubation in solution of 4 M GdnHCl, some amount of inactivated actin is still present. Therefore, it was still possible to record I_{int} at a concentration of GdnHCl up to 4 M. The decay lifetime of the initially inactivated actin after incubation for 24 h in 4 M GdnHCl, as was expected, retained the value characteristic of inactivated actin.

Kinetics of Actin Unfolding by GdnHCl. The fact that the kinetics of actin RTP changes when protein at a relatively low concentration (0.8 mg/mL) is transferred to 1.8 M GdnHCl confirms the conclusion that the essential unfolding precedes formation of inactivated actin. These experiments also suggest that integral intensity of actin RTP is equal to zero in this essentially unfolded state U*. Under these conditions, a weak RTP can be recorded only for several minutes after beginning the measurements (an additional 7 min were required for oxygen removal). During further incubation in solution of 1.8 M GdnHCl the integral intensity of RTP gradually increases and in 70 min reaches the maximum value that is close to that of inactivated actin. Hence, the increase of RTP intensity reflects the process of inactivated actin formation from the essentially unfolded state U*. If this formation had been the single-stage process "all or nothing", the intensive characteristic of the system, such as $<\tau>$, would have been equal to the corresponding value of inactivated actin in the whole range of I_{int} changes from zero to its maximal value. However, in reality this is not so. The value of $<\tau>$ increases in a symbate way with I_{int}. The reason for this is quite clear. Inactivated actin, a homogeneous associate consisting of 15 macromolecules of actin, could not be formed from the essentially unfolded state of actin by the single-stage transition U* → I. Inactivated actin is formed from the unfolded state U* by a gradual increase of associate:

$$U^* \rightarrow I_1 \cdots \rightarrow I_n \rightarrow \cdots I_{15} \qquad (6)$$

which is accompanied by an increase of rigidity of this associate.

Although evident, this scheme has not been previously proven experimentally. The dependence of the rate of inactivated actin formation on the concentration of protein in solution is an additional confirmation of the correctness of this scheme. Figure 4A,B shows that the time needed to reach maximal values of I_{int} and $<\tau>$ of RTP, corresponding to that of inactivated actin, decreases with the increase of protein concentration. It suggests facilitation of complexation with increase of the protein amount in solution. When protein concentration is 1.5 mg/mL and higher, the amount of inactivated actin having a rigid structure, which allows valid RTP recording, is accumulated as early as within 7 min after the beginning of protein incubation in 1.8 M GdnHCl. The high maximum values of τ_1, τ_2, and $<\tau>$ of RTP of actin incubated in 1.8 M GdnHCl suggest that the slow intramolecular mobility of inactivated actin is significantly lower than that of the native and completely unfolded states of the protein (Table 1, Figure 4B). Thus, the data obtained by RTP confirm the earlier proposed scheme of the actin folding-unfolding. These data also demonstrate that the U* → I transition is a gradual process of increasing mass of associate and allows the characterization of the slow intramolecular mobility of actin in different structural states.

ACKNOWLEDGMENT

The authors are very grateful to Mrs. Patricia Reynolds for careful reading and editing of the manuscript.

REFERENCES

1. Carrell, R. W., and Gooptu, B. (1998) *Curr. Opin. Struct. Biol. 8*, 799−809.
2. Kelly, J. W. (1997) *Structure 5*, 595−600.
3. Harper, J. D., and Lansbury, P. T., Jr. (1997) *Annu. Rev. Biochem. 66*, 385−407.
4. Koo, E. H., Lansbury, P. T., Jr, and Kelly, J. W. (1999) *Proc. Natl. Acad. Sci. U.S.A. 96*, 9989−9990.
5. Hashimoto, M., and Masliah, E. (1999) *Brain Pathol. 9*, 707−720.
6. Uversky, V. N., Talapatra, A., Gillespie, J. R., and Fink, A. L. (1999) *Med. Sci. Monitor 5*, 1001−1012.
7. Uversky, V. N., Talapatra, A., Gillespie, J. R., and Fink, A. L. (1999) *Med. Sci. Monitor 5*, 1238−1254.
8. Fink, A. L. (1998) *Fold. Des. 3*, R9−23.
9. Schein, C. H. (1989) *Biotechnology 7*, 1141−1149.
10. Frankel, S., Condeelis, J., and Leinwand, L. (1990) *J. Biol. Chem. 265*, 17980−17987.
11. Wetzel, R. (1992) in *Protein Engineering. A Practical Approach.* (Rees, A. R, Sternberg, A. R., and Wetzel, R., Eds.) pp 191−219, IRL Press, Oxford.
12. Wetzel, R. (1994) *Trends Biotechnol. 12*, 193−198.
13. Speed, M. A., Wang, D. I., and King, J. (1996) *Nat. Biotechnol. 14*, 1283−1287.
14. Nienhaus, G. U., and Yang, R. D. (1996) *Encycl. Appl. Phys. 15*, 163−184.
15. Hammes-Schiffer, S. (2002) *Biochemistry 41*, 13335−13343.
16. Johnson, L. N. (1985) in *Modern Physical Methods in Biochemistry*. Pt. A. (Neuberger, B., and Deenen, V., Eds.) pp 347−415, Elsever Science Publishers, Amsterdam.
17. Effink, M. R., and Ghiron, C. A. (1977) *Biochemistry 16*, 5546−5551.
18. Lakovitch, J. R., and Weber, G. (1980) *Biophys. J. 32*, 591−601.
19. Mazhul', V. M., Zaitseva, E. M., and Shcherbin, D. G. (2000) *Biophysics 45*, 935−959.
20. Strambini, G. B. (1989) *J. Mol. Liq. 42*, 155−163.
21. Subramaniam, V., Gafni, A., and Steel, D. G. (1996) *IEEE J. Sel. Top. Quantum Electron. 2*, 1107−1114.
22. Vanderkooi, J. M. (1992) in *Topics in Fluorescence Spectroscopy* (Lakowitcz, J. R., Ed.) pp 113−136, Plenum Press, New York, London.
23. Gonnelli, M., and Strambini, G. B. (1995) *Biochemistry 34*, 13847−13857.
24. Shauerte, J., Steel, D. G., and Gafni, A. (1997) *Methods Enzymol. 278*, 49−71.
25. Sun, L., Kantrowitz, E. R., and Galley, W. C. (1998) *Proc. SPIE 3256*, 236.
26. Mazhul', V. M., Zaitseva, E. M., Mitskevich, L. G., Fedurkina, N. V., and Kurganov, B. I. (1999) *Biophysics 44*, 975−987.
27. Gonnelli, M., and Strambini, G. B. (1993) *Biophys. J. 65*, 131−137.
28. Fisher, C. J., Shauere, J. A., Wisser, K. C., Gafni, A., and Steel, D. G. (2000) *Biochemistry 39*, 1455−1461.
29. Kabsch, W., Mannherz, H. G., Suck, D., Pai, E. F., and Holmes, K. C. (1990) *Nature 347*, 37−44.
30. Lehrer, S. L., and Kerwar, G. (1972) *Biochemistry 11*, 1211−1217.
31. Turoverov, K. K., Biktashev, A. G., Khaitlina, S. Yu., and Kuznetsova, I. M. (1999) *Biochemistry 38*, 6261−6269.
32. Nagy, B., and Jencks, W. P. (1962) *Biochemistry 1*, 987−996.
33. Nagy, B., and Strzelecka-Golaszewska, H. (1972) *Arch. Biochem. Biophys. 150*, 428−435.

34. Strzelecka-Golaszewska, H., Nagy, B., and Gergely, J. (1974) *Arch. Biochem. Biophys. 161*, 559−569.
35. Contaxis, C. C., Bigelow, C. C., and Zarkadas, C. G. (1977) *Can. J. Biochem. 55*, 325−331.
36. Kuznetsova, I. M., Khaitlina S. Yu., Konditerov, S. N., Surin, A. M., and Turoverov, K. K. (1988) *Biophys. Chem. 32*, 73−78.
37. Bertazzon, A., Tian, G. H., Lamblin, A., and Tsong, T. Y. (1990) *Biochemistry 29*, 291−298.
38. Le Bihan, T., and Gicquaud, C. (1993) *Biochim. Biophys. Res. Commun. 194*, 1065−1073.
39. Schuler, H., Lindberg, U., Schutt, C. E., and Karlsson, R. (2000) *Eur. J. Biochem. 267*, 476−486.
40. Kuznetsova, I. M., Turoverov, K. K., and Uversky, V. N. (1999) *Protein Pept. Lett. 6*, 173−178.
41. Kuznetsova, I. M., Biktashev, A. G., Khaitlina, S. Yu., Vassilenko, K. S., Turoverov, K. K., and Uversky, V. N. (1999) *Biophys. J. 77*, 2788−2800.
42. Turoverov, K. K., Verkhusha, V. V., Shavlovsky, M. M., Biktashev, A. G., Povarova, O. I., and Kuznetsova, I. M. (2002) *Biochemistry 41*, 1014−1019.
43. Kuznetsova, I. M., Stepanenko, O. V., Stepanenko, O. V., Povarova, O. I., Biktashev, A. G., Verkhusha, V. V., Shavlovsky, M. M., and Turoverov, K. K. (2002) *Biochemistry 41*, 13127−13132.
44. Horie, T., and Vanderkooi, J. M. (1982) *FEBS Lett. 147*, 69−73.
45. Strambini, G. B., and Lehrer, S. S. (1991) *Eur. J. Biochem. 159*, 645−651.
46. Pardee, J. D., and Spudich, J. A. (1982) *Methods Enzymol. 85*, 164−181.
47. Turoverov, K. K., Khaitlina, S. Yu., and Pinaev, G. P. (1976) *FEBS Lett. 62*, 4−7.
48. Rees, M. K., and Young, M. (1967) *J. Biol. Chem. 242*, 4449−4458.
49. Garcia, M., and Sanz-Medel, A. (1986) *Anal. Chem. 58*, 1436−1440.
50. Munoz de la Pena, A., Duran-Meras, I., and Salinas, F. (1991) *Anal. Chem. Acta 255*, 351−357.
51. Mazhul', V. M., and Shcharbin, D. G. (1997) *Proc. SPIE 2980*, 487−495.
52. Mazhul', V. M., and Shcherbin, D. G. (1998) *Biophysics 43*, 431−437.
53. Fischer, C. J., Gafni, A., Steel, D. G., and Schauerte, J. A. (2002) *J. Am. Chem. Soc. 124*, 10359−10366.
54. Lee, Z., Lee, W. E., and Galley, W. C. (1989) *Biophys. J. 56*, 361−367.
55. Lee, Z., Lee, W. E., and Galley, W. C. (1992) *Biophys. J. 61*, 1364−1371.

BI0350295